

## Linking Alterations in Tau Phosphorylation and Cleavage during Neuronal Apoptosis\*

Received for publication, July 20, 2004, and in revised form, October 7, 2004  
Published, JBC Papers in Press, October 8, 2004, DOI 10.1074/jbc.M408186200

Armelle Rametti, Françoise Esclaire, Catherine Yardin, and Faraj Terro†

From the EA 3842, Homéostasie Cellulaire et Pathologie, Department of Histology and Cell Biology,  
Faculty of Medicine, Limoges 87025, France

Neurofibrillary tangles (NFTs) are classic lesions of Alzheimer's disease. NFTs are bundles of abnormally phosphorylated tau, the paired helical filaments. The initiating mechanisms of NFTs and their role in neuronal loss are still unknown. Accumulating evidence supports a role for the activation of proteolytic enzymes, caspases, in neuronal death observed in brains of patients with Alzheimer's disease. Alterations in tau phosphorylation and tau cleavage by caspases have been previously reported in neuronal apoptosis. However, the links between the alterations in tau phosphorylation and its proteolytic cleavage have not yet been documented. Here, we show that, during staurosporine-induced neuronal apoptosis, tau first undergoes transient hyperphosphorylation, which is followed by dephosphorylation and cleavage. This cleavage generated a 10-kDa fragment in addition to the 17- and 50-kDa tau fragments previously reported. Prior tau dephosphorylation by a glycogen synthase kinase-3 $\beta$  inhibitor, lithium, enhanced tau cleavage and sensitized neurons to staurosporine-induced apoptosis. Caspase inhibition prevented tau cleavage without reversing changes in tau phosphorylation linked to apoptosis. Furthermore, the microtubule depolymerizing agent, colchicine, induced tau dephosphorylation and caspase-independent tau cleavage and degradation. Both phenomena were blocked by inhibiting protein phosphatase 2A (PP2A) by okadaic acid. These experiments indicate that tau dephosphorylation precedes and is required for its cleavage and degradation. We propose that the absence of cleavage and degradation of hyperphosphorylated tau (due to PP2A inhibition) may lead to its accumulation in degenerating neurons. This mechanism may contribute to the aggregation of hyperphosphorylated tau into paired helical filaments in Alzheimer's disease where reduced PP2A activity has been reported.

Tau is a microtubule-associated protein largely expressed in neurons and is predominantly found in axons (1). Tau interacts with microtubules via specific microtubule-binding domains and promotes their assembly and stability (for review see Ref. 2). Tau is regulated by differential phosphorylation of specific serine and threonine residues. In general, increases in tau phosphorylation correlate inversely with its ability to bind and stabilize microtubules (3, 4). Protein phosphatases, especially

protein phosphatase 2A (PP2A)<sup>1</sup> and protein phosphatase 1, were shown to regulate the activities of several protein kinases that phosphorylate tau (5). Among these kinases, glycogen synthase kinase-3 and particularly the glycogen synthase kinase-3 $\beta$  isoform have been most implicated in tau hyperphosphorylation (6). Tau, in its hyperphosphorylated form, is the major component of PHF, the building block of neurofibrillary tangle lesions observed in brains from patients with Alzheimer's disease (AD) (7–9).

Apoptosis, a form of cell death is classically divided into three sequential phases: the induction phase, the commitment phase, and the execution phase, which is considered as the final stage. During the execution phase, all morphological hallmarks of apoptosis occur, and the cell loses viability. Once this phase begins, death becomes irreversible (10). This phase is initiated by the activation of several subsets of proteases, including caspases, calpains, cathepsin D, and proteasomes (for review see Ref. 11). Proteolysis of cellular proteins is one of the critical mechanisms of apoptosis (12). Some of these proteins are cytoskeletal proteins such as actin, fodrin, and gelsolin (13, 14). Tau and other cytoskeletal proteins play an important role in facilitating the cytoskeletal reorganization that occurs during apoptotic cell death (15). Given its role in the stabilization of microtubules, it is therefore not surprising that changes in tau phosphorylation states (which alter its binding to microtubules) play an important role in cell fate. In fact, several studies reported that tau is hyperphosphorylated during neuronal apoptosis and that this phosphorylation occurs in a site-specific manner and results in decreased tau binding to microtubules (16–18). Using primary neuronal cultures from embryonic rat cortices, Lesort *et al.* (19) demonstrated that, *in situ*, tau was dephosphorylated at the Tau-1 epitope in apoptotic neurons. This finding was then confirmed in apoptosis of human cell lines (16, 20) and cultured rat cerebellar granule cells (18). In addition, in a more detailed study, Mills *et al.* (20) demonstrated that in individual PC-12 cells undergoing apoptosis, tau dephosphorylation takes place early in the execution phase of apoptosis. Using cerebellar granule cell cultures deprived of potassium or serum, Canu *et al.* (18) showed that tau dephosphorylation at the Tau-1 epitope is associated with tau cleavage giving rise to a final 17-kDa dephosphorylated tau fragment, which resulted from tau proteolysis by calpain. Whether tau dephosphorylation preceded or followed tau cleavage was not investigated.

To understand the opposing data concerning the modifications in tau phosphorylation during neuronal apoptosis and to

\* This work was supported by the Conseil Régional du Limousin and the Association France-Alzheimer. The costs of publication of this article were defrayed in part by the payment of page charges. This article must therefore be hereby marked "advertisement" in accordance with 18 U.S.C. Section 1734 solely to indicate this fact.

† To whom correspondence should be addressed. Tel.: 33-5-55-43-58-33; Fax: 33-5-55-43-58-93; E-mail: faraj.terro@unilim.fr.

<sup>1</sup> The abbreviations used are: PP2A, protein phosphatase 2A; AD, Alzheimer's disease; PHF, paired helical filament; OKA, okadaic acid; TRITC, tetramethylrhodamine isothiocyanate; DAPI, 4',6-diamino-2-phenylindole; Boc-D-FMK, *t*-butoxycarbonyl-Asp (OMe)-fluoromethyl ketone; Tau FL, full-length tau.

situate these modifications in relation to tau cleavage and apoptosis, we analyzed the sequential modifications of tau phosphorylation during apoptotic processes. We also assessed the effects of tau phosphorylation/dephosphorylation on its cleavage and on the vulnerability of neurons to apoptosis.

#### EXPERIMENTAL PROCEDURES

**Material**—To assess tau phosphorylation, the following antibodies were used: AT-8, AT-180, and AT-270 were purchased from Innogenetics (Belgium); Tau-1 from Chemicon and distributed by Euromedex (France); and T46, AD-2, 12E8, and TauC3 monoclonal antibodies were kindly provided by Dr. V. M.-Y. Lee (University of Pennsylvania), Dr. C. Mourtou-Gilles (Montpellier, France), Dr. P. Seubert (San Francisco, CA), and Prof. L. I. Binder (Chicago, IL), respectively. According to the residue numbering of the longest human tau isoform of 441 amino acids (21), Tau-1 recognizes tau only when serines 195, 198, 199, and 202 are not phosphorylated. AT-8 recognizes tau when phosphorylated at Ser<sup>202</sup> and Thr<sup>205</sup>. AT180 recognizes tau protein when phosphorylated at threonines 231 and 235. AT-270 recognizes tau phosphorylated at Thr<sup>181</sup>. AD-2 recognizes a phosphorylated epitope, including Ser<sup>396</sup>, and, to a lesser extent, Ser<sup>404</sup> (22). 12E8 detects tau phosphorylated at Ser<sup>262</sup> and to a lesser extent at Ser<sup>356</sup> (23). T46 recognizes an epitope located at the C terminus (residues 404–441). The phospho-independent antibody Tau-5 (residues 210–230) was purchased from Calbiochem. Polyclonal anti-global tau antibody (Tau-G) and anti-actin antibody were obtained from Sigma. TauC3 antibody specifically recognizes residues 412–421 of tau cleaved at Asp<sup>421</sup> (24). Staurosporine, LiCl, and okadaic acid (OKA) were purchased from Sigma. Unless otherwise indicated, all other reagents were purchased from Sigma.

**Cell Cultures**—Cortical cultures were prepared from embryonic Wistar rats (E17) as previously described (25).

**Induction and Assessment of Apoptosis**—Eight-day *in vitro* cultures were exposed to staurosporine, a well known trigger of apoptosis (26). Staurosporine (1 mM stock solution) was dissolved in Me<sub>2</sub>SO and kept in aliquots at –20 °C until use. Working solutions were prepared in bathing culture medium. To analyze time-dependent changes in tau phosphorylation occurring during staurosporine-induced apoptosis, cultures were exposed to a single dose of staurosporine (0.5  $\mu$ M) for different time periods (15, 30, and 45 min and 1, 2, 4, 6, 8, 16, and 24 h). Control cultures were incubated in bathing culture medium containing <0.1% vehicle Me<sub>2</sub>SO. Cells fixed with 4% paraformaldehyde were stained with the specific nuclear dye, 4',6'-diamino-2-phenylindole (DAPI). Nuclear staining was examined under epifluorescence microscope (Eclipse E-800, Nikon) using an appropriate filter. Cells with fragmented nuclei (three to four lobes) were considered apoptotic. At least 500 cells were assessed, and the percentage of apoptotic neurons was calculated.

**Role of Caspases in Tau Cleavage and Apoptosis**—To assess the involvement of caspases in tau cleavage and apoptosis, caspases were inhibited by 50 and 100  $\mu$ M pan caspase inhibitor, *t*-butoxycarbonyl-Asp (OMe)-fluoromethyl ketone (Boc-D-FMK) (Enzyme Systems Products, CA). Boc-D-FMK was added to cultures 2 h prior to and once during staurosporine exposure.

**Relationship between Tau Dephosphorylation and Cleavage**—Tau dephosphorylation was previously demonstrated to occur during the execution phase of apoptosis (20). To induce tau dephosphorylation, cultures were preincubated with 10 or 15 mM LiCl for 6 h. After two washes with minimum essential medium, apoptosis was induced by 0.5  $\mu$ M staurosporine for 3 h, and tau cleavage was analyzed by Western blot. Tau dephosphorylation and cleavage were also assessed in cultures exposed for different time periods (1, 2, 4, 6, 8, and 12 h) to 1  $\mu$ M colchicine. Colchicine is a toxin known to depolymerize microtubules, to destabilize the cytoskeleton, and to dephosphorylate tau (27, 28). Colchicine exposure was also carried out with 25 or 50 nM OKA for 8 h.

**Tau Fractionation**—Fractionation was performed as described by Jenkins *et al.* (29). To determine whether tau cleavage occurred during fractionation into soluble and bound tau, fractionation was carried out at 37 °C for 10 and 20 min in buffer with or without the pan caspase inhibitor, Boc-D-FMK. This buffer also contained protease and phosphatase inhibitor mixtures. Protein extracts were then mixed with 2 $\times$  Laemmli sample buffer and heat-denatured for 8 min at 90 °C.

**Western Blot**—Cells in 35-mm Petri dishes were washed twice with phosphate-buffered saline, and total proteins were extracted by scraping the cells in 100  $\mu$ l of modified Laemmli sample buffer (60 mM Tris, pH 6.8, 2% SDS, 10% glycerol, 0.5 mM EDTA, 1 mM EGTA, phosphatase inhibitor mixture I, protease inhibitor mixture I (Sigma), 0.5 mM sodium orthovanadate, 1  $\mu$ M okadaic acid, 1  $\mu$ g/ml *N*-tosyl-L-phenylalanine chloromethyl ketone, 1  $\mu$ g/ml *N* $^{\alpha}$ -*p*-tosyl-L-lysine chloromethyl ke-

tone, 20 mM sodium fluoride, 1  $\mu$ M phenylmethylsulfonyl fluoride). Lysates were then sonicated on ice and centrifuged. The resulting supernatants were collected, and protein concentrations were determined by BCA assay (Pierce). Samples were mixed with 50 mM dithiothreitol and 0.5%  $\beta$ -mercaptoethanol and heated at 90 °C for 5–8 min. Depending on the primary antibody used in Western blot, 25–50  $\mu$ g of total protein was separated by electrophoresis on 4–20% gradient SDS-acrylamide gels, transferred to polyvinylidene difluoride membranes (Millipore), and probed with the indicated antibodies. After incubation with appropriate horseradish peroxidase-conjugated secondary antibodies (DAKO, Denmark), Western blots were developed using enhanced chemiluminescence (ECL) (Amersham Biosciences). Western blots were analyzed by densitometry (Bio-Rad gel doc 2000 imaging system). Phosphorylated and dephosphorylated tau levels (detected by phospho-dependent anti-tau antibodies) were normalized to total tau (detected by Tau-5 antibody), which in turn was normalized to  $\beta$ -actin.

**Immunohistochemistry**—Cell cultures were fixed in 4% paraformaldehyde in phosphate-buffered saline for 20 min at room temperature. Double immunostainings were carried out using AT-8 and Tau-1 antibodies. These two monoclonal antibodies were simultaneously revealed by goat secondary antibodies (Clinisciences, France), which recognize mouse IgG subclasses. AT-8 (IgG<sub>1</sub> $\kappa$ ) was revealed by an anti-IgG1 antibody coupled to TRITC and Tau-1 (IgG<sub>2a</sub>) with an anti-IgG<sub>2a</sub> antibody coupled to fluorescein isothiocyanate. To determine whether apoptosis-altered localization of dephosphorylated tau was due to tau cleavage or to its dephosphorylation, we carried out double immunostainings with the polyclonal anti-total (phosphorylation-independent epitope) tau antibody, Tau-G, and with the anti-dephosphorylated tau antibody, Tau-1. Tau staining with Tau-G was detected by a goat anti-rabbit IgG antibody coupled to TRITC, and labeling with Tau-1 was revealed by goat anti-mouse IgG antibody coupled to fluorescein isothiocyanate (Jackson Laboratories). To visualize apoptosis, all immunostainings were combined to the nuclear staining with DAPI. Image acquisition was monitored with a charge-coupled device camera (Photonic science) using Visiolab 2000 software (Biocom, France). Data were statistically analyzed using Student's *t* test and considered significantly different when *p* < 0.05.

#### RESULTS

**During Neuronal Apoptosis, for the Majority of Phospho-Tau Epitopes Analyzed, an Increase in Tau Phosphorylation Precedes Tau Dephosphorylation and Cleavage**—It is largely admitted that tau phosphorylation increases during neuronal apoptosis (16, 17). On the other hand, data from several previous studies (18–20) demonstrated that apoptosis is more closely associated with increased tau dephosphorylation. To understand these apparently conflicting data, we analyzed the alterations in tau phosphorylation during the time course of neuronal apoptosis. Western blots shown in Fig. 1 were carried out using proteins extracted in modified Laemmli sample buffer as described under “Experimental Procedures.” In control cultures all anti-tau antibodies detected a 55- to 56-kDa major band and a 60- to 62-kDa minor band. These bands represent uncleaved tau proteins (full-length tau = Tau FL) (Fig. 1A). Only the 55- to 56-kDa band was semi-quantified by densitometry. Western blots using anti-phosphorylated tau antibodies, AT-8, AT-180, AT-270, and AD-2 showed that 0.5  $\mu$ M staurosporine induced transient increases in phosphorylated tau. The changes in tau phosphorylation depended upon the phosphorylation epitope analyzed. At AT-8, AT-180, and AT-270 epitopes, the increase in phosphorylated tau occurred after 15 min of staurosporine exposure (Fig. 1A) and peaked after 45 min of exposure (see Fig. 1B for densitometric analysis of Western blots presented in Fig. 1A). For example, at the AT-8 epitope, phosphorylated tau comprised 175% of controls following 45-min staurosporine exposure. Similarly, for the AD-2 epitope, the increase in phosphorylated tau was observed at 15 min, but peaked only at 2-h staurosporine exposure. For all tau phosphorylation epitopes analyzed, except at the 12E8 epitope, a decrease in phosphorylated tau was observed after the initial increase. For the AT-8 epitope, this decrease occurred 1 h after staurosporine exposure (compared with the increase seen at 45

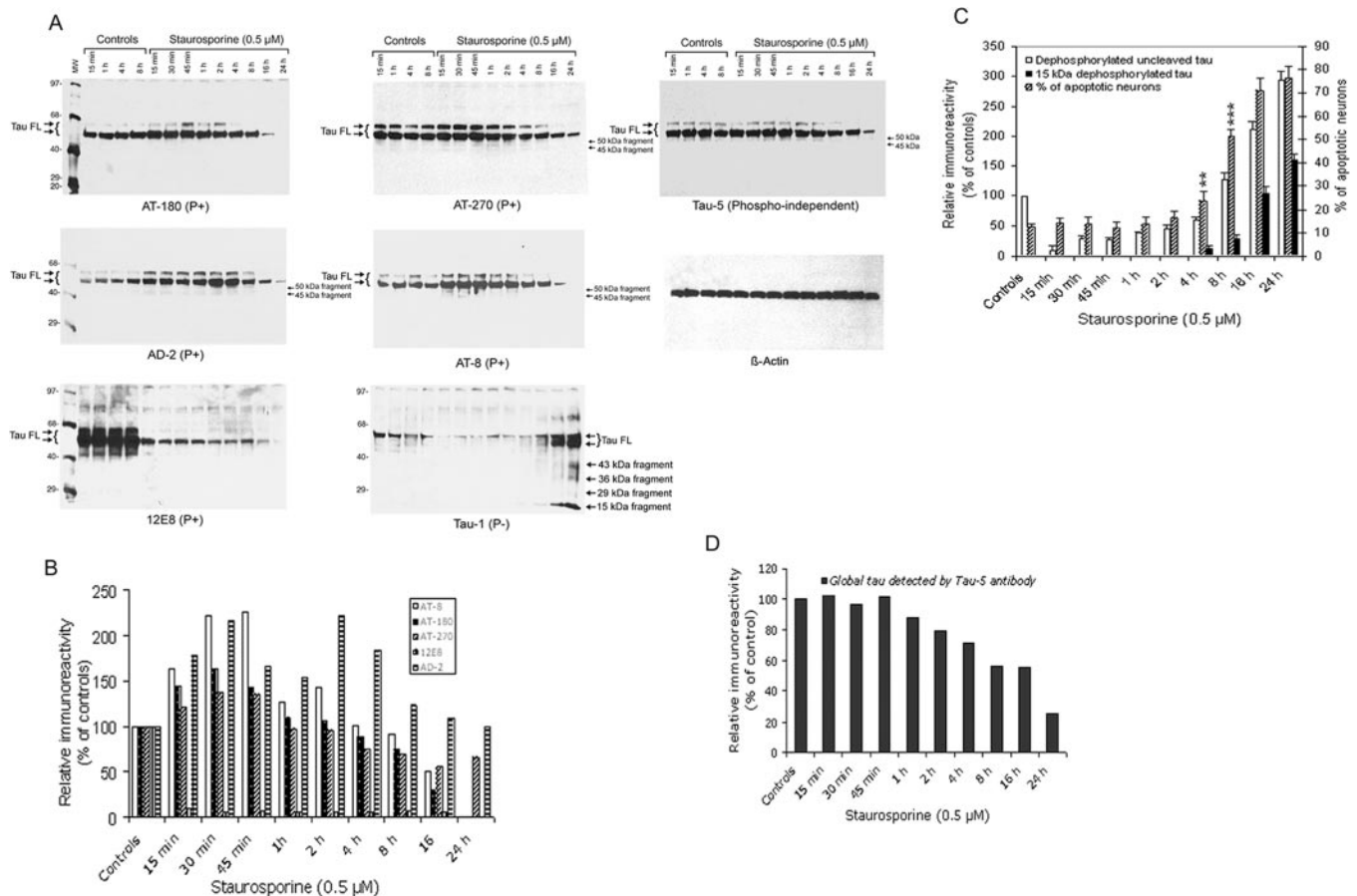


**FIG. 1. Tau phosphorylation during staurosporine-induced apoptosis.** *A*, Western blot analysis using monoclonal antibodies directed against specific tau phosphorylation epitopes. Antibodies recognize tau phosphorylated (*P*+) or dephosphorylated (*P*−) at the mentioned epitopes. Total tau was detected by Tau-5 antibody. *B*, densitometric analysis of Western blots using anti-phosphorylated tau antibodies shown in *A*. For the majority of tau phosphorylation epitopes examined, staurosporine transiently increased phosphorylated tau. At the opposite, phosphorylation at the 12E8 epitope Ser<sup>262</sup> was decreased. *C*, densitometric analysis of Western blots using anti-dephosphorylated tau antibody and quantification of apoptosis. Dephosphorylated tau decreased during staurosporine exposure (up to 4 h) and then increased. This increase in dephosphorylated tau was associated with tau cleavage, which led to a laddering of tau fragments, including a final 15-kDa product. For each time point, the corresponding percentage of apoptotic neurons was indicated. Levels of the 15-kDa fragment were correlated with the percentages of apoptosis. In densitometric analyses of each Western blot, control bars represent the mean densities of four controls at 15 min, 1 h, 4 h, and 8 h. *D*, total tau detected by Tau-5 antibody (Western blot in *A*) decreased during staurosporine exposure in a time-dependent manner. Immunoreactivities are expressed as percentages of controls. *Tau FL* = full-length tau. \*\*,  $p < 0.01$ ; \*\*\*,  $p < 0.001$  compared with apoptosis in control cultures.

min). At 24-h staurosporine exposure, no AT-8 immunoreactivity was detected. These variations (increase and then decrease) in phosphorylated tau were then confirmed by Western blots using Tau-1 antibody, which recognizes tau only when serines 195, 198, 199, 202, and threonine 205 are not phosphorylated. Dephosphorylated tau detected by Tau-1 antibody showed an early (within 15-min staurosporine exposure compared with controls) decrease and then started to increase after 1 h and continued until 24-h staurosporine exposure (Fig. 1, *A* and *C*). In contrast to what was observed for the majority of tau phosphorylation epitopes, staurosporine induced a decrease in tau phosphorylation at the 12E8 epitope. This decrease was observed at 15-min staurosporine exposure and was maintained even when exposure to staurosporine was prolonged until 24 h (Fig. 1, *A* and *B*).

**Tau Cleavage Is Associated with Its Dephosphorylation and Is Correlated with the Occurrence of Apoptotic Features**—Western blots using anti-dephosphorylated tau antibody, Tau-1, showed that tau dephosphorylation increased greatly following 8-h staurosporine exposure compared with 45-min exposure (Fig. 1*C*). This increase was associated with tau cleavage, which coincided with the occurrence of morphological features of apoptosis (chromatin fragmentation, cell body retraction, and loss of neurite outgrowth, see below). Following 8-, 16-, and

24-h staurosporine exposures, Tau-1 detected a laddering of dephosphorylated tau, including a final tau fragment of ~15 kDa (Fig. 1*A*). This fragment was already detected following 4-h exposure, and its levels increased with the percentages of apoptotic neurons (Fig. 1*C*). Apoptosis was 23.6% ( $p < 0.01$ ), 51.2% ( $p < 0.001$ ), and 70.8%, following 4-, 8-, and 16-h staurosporine exposures, respectively, and the corresponding intensity values of the 15-kDa fragment were 14 (arbitrary units), 28, and 106. There was no correlation between the increase in tau phosphorylation and the percentage of apoptotic neurons.

Chung *et al.* (30) demonstrated that tau cleavage occurred during staurosporine-induced neuronal apoptosis of cultured cortical neurons. This cleavage led to a 50-kDa fragment, which represented residues 1–421. In addition, using an acellular system, these authors demonstrated that recombinant tau protein could be cleaved by caspase-3 at Asp<sup>421</sup>. These data were recently confirmed by Gamblin *et al.* (24). In that study, tau cleavage was reported to occur during apoptosis of cultured neurons exposed to amyloid  $\beta$ -(1–42). This cleavage generated a truncated tau protein that lacked its 20 C-terminal amino acids. The truncated protein corresponded to the 50-kDa fragment and had an increased ability to assemble into filaments compared with wild-type tau. Both studies showed that the 50-kDa fragment could be detected



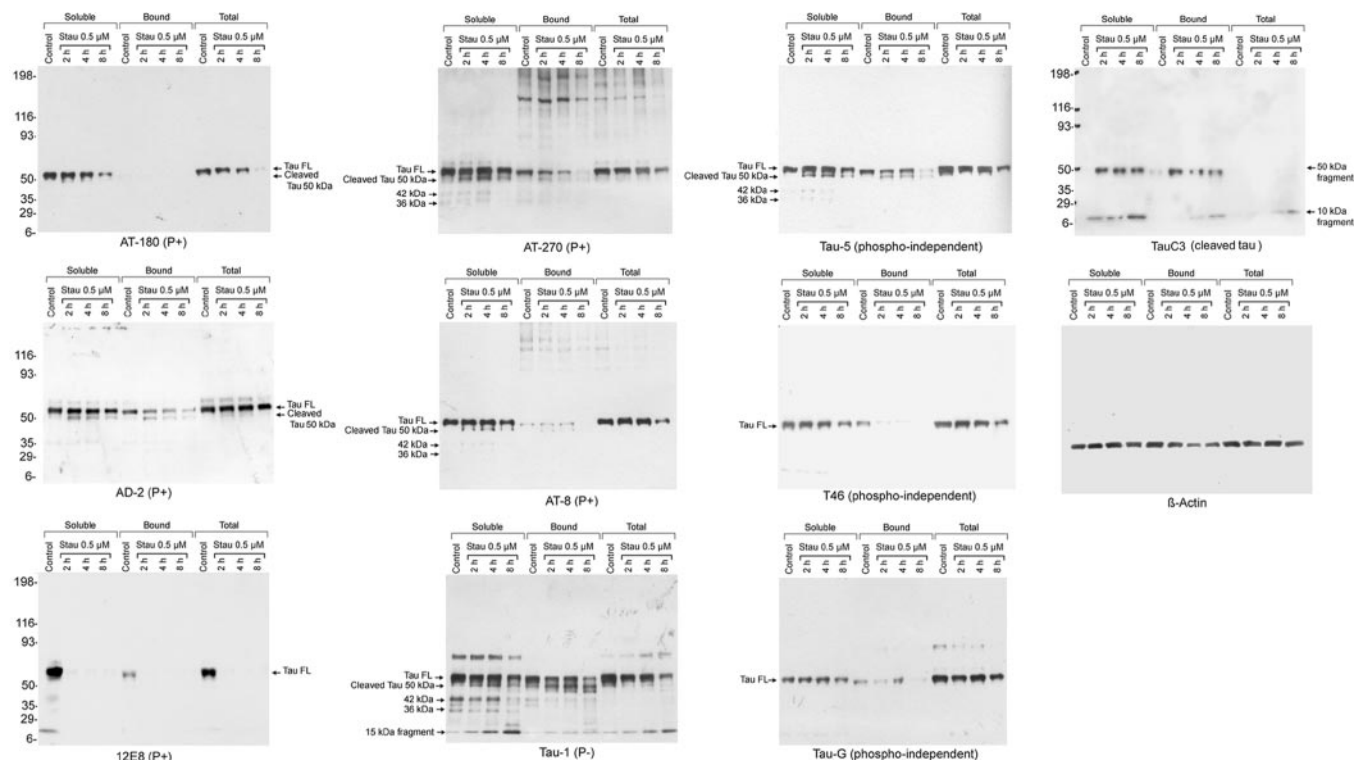


**FIG. 2. Analysis of tau cleavage and distribution in total, soluble, and bound fractions by Western blot.** In the total fraction: antibodies specific for phosphorylated tau (*P*+) and total tau (phospho-independent) failed to detect tau fragments. Phospho-independent tau antibodies Tau-5, T46, and Tau-G showed that staurosporine decreased total tau. Western blot using Tau-1 (*P*−) antibody shows a time-dependent dephosphorylated tau decrease and detected increasing levels of the 15-kDa fragment. TauC3 mainly detected a fragment of ~10 kDa after 4- and 8-h staurosporine exposure. In bound and soluble fractions: Phosphorylated tau and total tau increased after 2-h staurosporine exposure and then decreased after 8 h in the soluble fraction, whereas they constantly decreased in the bound fraction. Antibodies directed against phosphorylated, dephosphorylated (Tau-1), and phospho-independent tau (Tau-5) detected the 50-kDa fragment mainly in the soluble fraction. Tau-1 also detected 42- and 36-kDa fragments in both control and staurosporine-exposed cultures. TauC3 antibody detected 50-kDa and 10-kDa fragments both in soluble and bound fractions. 12E8 antibody showed decreased phosphorylated tau in soluble, bound, and total fractions.

by Tau-5 antibody, which reacts with residues 210–230 of tau independently of its phosphorylation states. This fragment was also specifically detected by TauC3, a monoclonal anti-cleaved tau antibody directed against residues 412–421 (24). In our study, when Western blots were carried out using 50  $\mu$ g of total cellular proteins extracted with modified Laemmli buffer, we detected a faint 45-kDa tau fragment with anti-phosphorylated tau antibody AD-2 within 15 min of staurosporine exposure (Fig. 1A). Anti-phosphorylated tau antibody, AT-8, and anti-phospho-independent tau antibody, Tau-5, barely detected a 50-kDa tau fragment, by contrast with what was reported by Chung *et al.* (30) and Gamblin *et al.* (24) who clearly detected the 50-kDa fragment.

In accordance with data reported by Canu *et al.* (18), we showed that only the anti-dephosphorylated tau antibody (Tau-1) was able to detect a sharp ladder of apoptosis-generated fragments, mainly a 15-kDa tau fragment (Fig. 1A) (17 kDa for Canu *et al.*). When normalized to actin, total tau detected by Tau-5 decreased time-dependently during staurosporine exposure (Fig. 1D).

We then tried to understand why we failed to detect sharp tau fragments with phospho-dependent and phospho-independent tau antibodies as previously described (24, 30). In particular, we investigated whether this result could be to differences under “Experimental Procedures” used in the different studies. Western blots presented in Fig. 1 of the present work were carried out in modified Laemmli sample buffer containing 2% ionic detergent SDS and phosphatase and protease inhibitors. Chung *et al.* (30) used Laemmli sample buffer without phosphatase and protease inhibitors, whereas Gam-

blin *et al.* (24) carried out cell extracts in stabilizing buffer that contained 1% non-ionic detergent Triton and a small amount of SDS (0.1%). The difference between the buffer that we used and the buffer used by Chung *et al.* is the presence of protease and phosphatase inhibitors. We first performed Western blots on cells lysed with Laemmli buffer without protease and phosphatase inhibitors. However, we again failed to observe sharp and easily detectable tau fragments with anti-phospho-independent and phospho-dependent tau antibodies, as described by Chung *et al.* (data not shown). We then used a buffer containing Triton as detergent and protease and phosphatase inhibitors to carry out cell extracts as described by Jenkins *et al.* (29). This protocol was used for tau fractionation (soluble and bound tau fractions) by incubating cultures in extraction buffer for 10 min at 37 °C. Fractions were then mixed with 2 $\times$  Laemmli sample buffer (v/v) and heat-denatured. In parallel we lysed cells with modified Laemmli buffer (used above) to obtain the total fraction. Tau phosphorylation and cleavage were then analyzed in soluble, bound, and total fractions. In the total fraction, neither anti-phospho-tau antibodies (AT-180, AT-8, AT-270, AD-2, and 12E8), nor anti-phospho-independent tau (total tau) antibodies (Tau-5, T46, and Tau-G) were able to detect sharp tau fragments during 0.5  $\mu$ M staurosporine-induced apoptosis (Fig. 2). Western blots using anti-phospho-independent antibodies, Tau-5, T46, and Tau-G revealed that total tau decreased time dependently (2-, 4-, and 8-h exposure) during staurosporine-induced apoptosis. In addition, we analyzed tau cleavage by TauC3 antibody, which specifically detects the 50-kDa fragment. In the total fraction, this antibody detected very few 50-kDa fragments even after 16-h stauro-

porine exposure, thereby confirming what was seen with anti-total tau antibodies. TauC3 also detected a 10-kDa fragment within 4-h staurosporine exposure. This fragment is different from the 15-kDa fragment detected by Tau-1 antibody, because there is no overlapping between tau epitopes recognized by these antibodies: TauC3 is directed against residues 412–421, whereas Tau-1 recognizes tau only when serines 195, 198, 199, 202, and threonine 205 are dephosphorylated. In summary, in the total fraction obtained from cultures exposed to 0.5  $\mu$ M staurosporine, only Tau-1 and TauC3 antibodies detected sharp tau fragments (several fragments with Tau-1; a 10-kDa fragment and a small amount of the 50-kDa fragment with TauC3), whereas antibodies that detect total tau showed only a clear decrease in the level of tau protein, which may reflect tau cleavage and degradation.

Analysis of tau distribution and cleavage by Western blot in the soluble and bound fractions showed that staurosporine increased soluble tau and decreased bound tau (Fig. 2). In contrast to what was observed in the total fraction, Western blots using anti-phosphorylated tau antibodies AT-180, AT-270, AT-8, and AD-2 did detect the 50-kDa fragment in the soluble fraction within 2-h staurosporine exposure. This fragment was also detected by the anti-total tau antibody, Tau-5, but not by T46 and Tau-G antibodies. T46 antibody recognizes tau residues 404–441. It failed to detect the 50-kDa fragment, probably because cleavage at Asp<sup>421</sup> suppressed recognition by this antibody. The epitopes recognized by Tau-G antibody are unknown. In addition to the 10-kDa fragment detected in the total fraction, TauC3 detected large levels (compared with levels found in the total fraction) of the 50-kDa fragment both in soluble and bound fractions. Tau-1 antibody detected a laddering of fragments, which included the 50-kDa fragment as well as 42- and 36-kDa fragments and the 15-kDa fragment. The 42- and 36-kDa fragments were not specific for staurosporine exposure, because they were detected in control extracts (Fig. 2). All fragments were mainly found in the soluble fraction. These experiments show that, depending on the protein extraction procedures used, the patterns observed for tau cleavage may differ.

The modified Laemmli sample buffer we used is more effective in blocking enzyme activities (*e.g.* protease inhibition) than buffers used in the other studies, because it contains a relatively high SDS concentration, which reduces proteins and irreversibly inactivates enzymes such as proteases. In our study, the presence of the 50-kDa fragment in the soluble fraction cannot be merely considered as an experimental artifact, because it is only associated with staurosporine exposure. However, we cannot exclude the possibility that, during fractionation, this cleavage may specifically occur in extracts from staurosporine-exposed cultures. This assumes that staurosporine activates caspases (and this has been largely demonstrated by numerous studies) and increases soluble tau as demonstrated here. Soluble tau could then be more effectively cleaved by staurosporine-activated caspases, which would explain why we easily detected the 50-kDa tau fragment. The fractionation buffer contains a mixture of protease inhibitors that may be ineffective in blocking staurosporine-activated caspases. To test this possibility, cultures were exposed to 0.5  $\mu$ M staurosporine or to 0.1% vehicle Me<sub>2</sub>SO for 2 h. Tau fractionation was then performed by incubating cultures in fractionation buffer for 10 and 20 min at 37 °C in the presence or not of 100  $\mu$ M pan caspase inhibitor Boc-D-FMK. Western blots were performed on cellular proteins obtained from soluble fractions (Fig. 3). When tau fractionation was carried out in buffer without Boc-D-FMK, TauC3 and Tau-5 antibodies detected high levels of the 50-kDa fragment in staurosporine-exposed

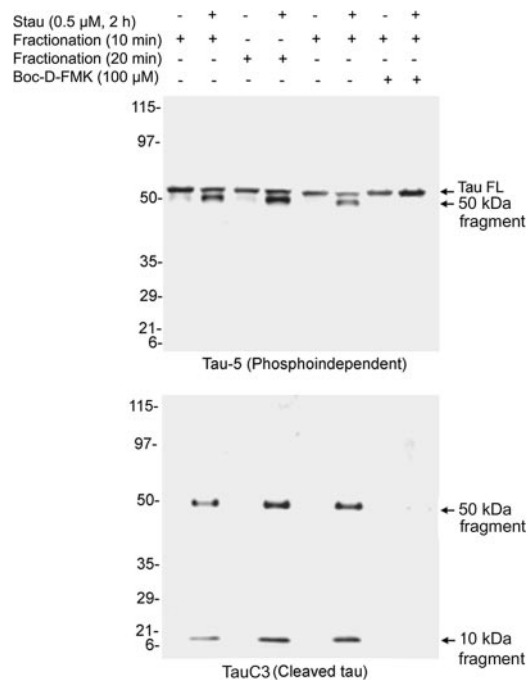


**FIG. 3. Analysis of tau cleavage during tau fractionation.** Proteins from soluble fractions obtained after 10- and 20-min extraction were analyzed by Western blot using anti-total tau antibody, Tau-5, and anti-cleaved tau, TauC3. Both antibodies detected high levels of the 50-kDa fragment in fractions from staurosporine-exposed cultures. In addition, TauC3 detected the 10-kDa fragment. These fragments augmented with prolonged extraction time, and their generation was prevented by caspase inhibition using 100  $\mu$ M Boc-D-FMK added during extraction.

cultures. TauC3 also detected the 10-kDa fragment. Levels of these fragments increased when fractionation time was prolonged to 20 min. Boc-D-FMK almost completely prevented generation of the 50- and 10-kDa fragments. These experiments clearly demonstrated that these tau fragments are generated at detectable levels during the extraction procedure. In our study, the absence of the 50-kDa fragment in the total fraction could be due to its presence at levels too low to be detected. This may result from its rapid degradation into smaller fragments, mainly the 10- and the 15-kDa fragments. Following these experimental problems, we thereafter used modified Laemmli sample buffer as the cell lysis buffer.

**Neurons with Altered Dephosphorylated Tau Distribution Are Apoptotic**—To assess the relationships between alterations in tau phosphorylation and occurrence of apoptotic features in individual neurons, we carried out simultaneous double immunostainings using the anti-phosphorylated tau antibody, AT-8, and the anti-dephosphorylated tau antibody, Tau-1 (Fig. 4). These mutually exclusive stainings were combined with nuclear staining by DAPI. In control cultures, all neurons showed a faint stain for dephosphorylated tau, mainly in neuron outgrowth (Fig. 4B), whereas a sharp and dominant staining for phosphorylated tau was found both in neuronal processes and cell bodies (Fig. 4C). In staurosporine-treated cultures, neurons with non-apoptotic nuclei (Fig. 4A') displayed enhanced AT-8 immunoreactivity (Fig. 4C'), whereas immunoreactivity of dephosphorylated tau was absent (Fig. 4B') compared with neurons from control cultures. In the majority of apoptotic neurons, dephosphorylated tau immunoreactivity increased in neuronal cell bodies and degenerating neurites (Fig. 4B'), whereas AT-8 immunoreactivity was absent (Fig. 4C').

Cell counting indicated that staurosporine induced an increase in the proportion of neurons with enhanced and altered distribution of dephosphorylated tau (Tau-1-positive

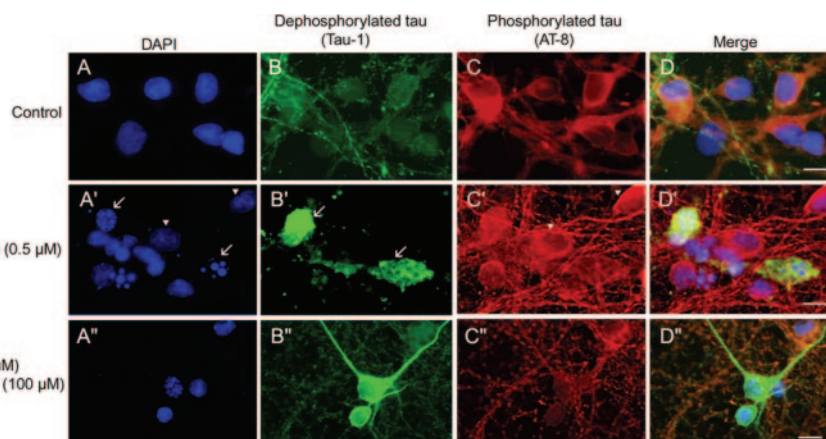


**FIG. 4. Analysis of tau phosphorylation in individual neurons during staurosporine-induced apoptosis.** Double immunostainings for phosphorylated (AT-8, red) and dephosphorylated (Tau-1, green) were combined with nuclear staining by DAPI (blue). In control cultures (A–D), phosphorylated tau was found both in cell bodies and neurites (C), whereas dephosphorylated tau was present mainly in neurites (B). In staurosporine-exposed cultures (A'–D'), the majority of apoptotic neurons were strongly stained for dephosphorylated tau both in cell bodies and degenerated neurites (B', arrows), whereas non-apoptotic neurons (A', arrowheads) exclusively displayed strong staining for phosphorylated tau (C', arrowheads). Caspase inhibition prevented neuronal apoptosis (A'') and had no effect on staurosporine-induced changes in tau phosphorylation (B'' and C''); protected neurons remained strongly stained for dephosphorylated tau (B''). Scale bars: 8  $\mu$ m.

neurons) compared with control cultures, in which <1% of neurons were Tau-1 positive. This increase was time-dependent (data not shown), and nearly all Tau-1-positive neurons had fragmented nuclei.

We then analyzed the links between apoptosis and alterations in tau phosphorylation and localization (enhanced dephosphorylated tau in neuronal cell bodies and degenerating axons). In cultures exposed to 0.5  $\mu$ M staurosporine for 8 h,  $62 \pm 3\%$  of apoptotic neurons displayed enhanced and altered localization in dephosphorylated tau immunoreactivity (Tau-1-positive) and  $38 \pm 4\%$  of apoptotic neurons were Tau-1-negative. None of the apoptotic neurons displayed phosphorylated tau immunoreactivity (at least at AT-8 epitope) indicating that about 38% apoptotic neurons were both AT-8- and Tau-1-negative. The absence of Tau-1 immunoreactivity in some apoptotic neurons may indicate that they are in advanced stages of apoptosis where degradation products (including tau fragments) of cell constituents were released in the culture medium. The few Tau-1-positive neurons found in control cultures (<1%) were also apoptotic (spontaneous apoptosis) suggesting that the alteration in dephosphorylated tau localization is a constant of neuronal apoptosis and does not depend on the nature of the trigger.

**The Alteration in Dephosphorylated Tau Distribution Linked to Apoptosis Is Due to Tau Cleavage and Not to Tau Dephosphorylation**—We further addressed the question of whether the alterations in the localization of dephosphorylated tau were linked to tau dephosphorylation itself or to its subsequent cleavage. Western blot analysis demonstrated that Tau-G antibody, which recognizes tau independently of its phosphorylation state, failed to detect apoptosis-generated tau fragments but did detect Tau FL (Fig. 2). Immunocytochemistry using Tau-G and Tau-1 combined with nuclear staining by DAPI revealed that >98% of Tau-1-positive apoptotic neurons were not stained with Tau-G (Fig. 5, C and D). This indicates that the abnormal distribution of tau in apoptotic neurons was merely due to its cleavage and degradation and not its dephosphorylation. These observations were then confirmed by additional experiments in which caspases were inhibited (see below). Caspase inhibition restored not only dephosphorylated full-length tau (due to inhibition of tau cleavage) but also the normal distribution of dephosphorylated tau, except that tau remained highly dephosphorylated in protected neurons (Fig. 4B'').

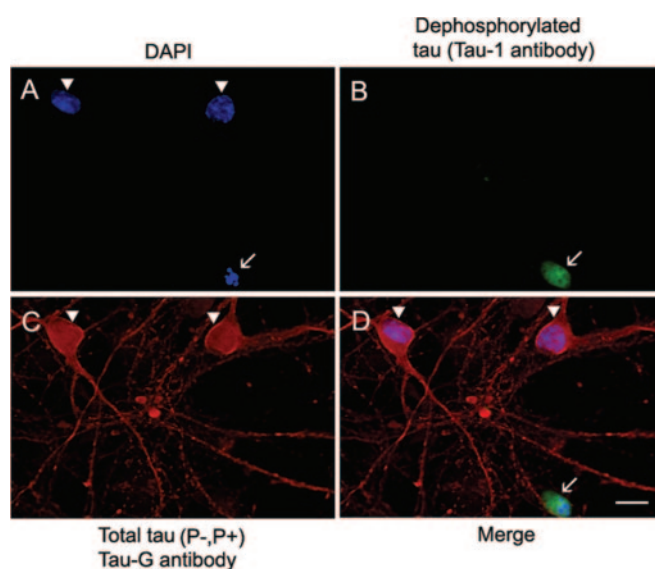


**FIG. 5. Tau localization during staurosporine-induced apoptosis.** Cultured cortical neurons were exposed to 0.5  $\mu$ M staurosporine for 8 h. Double immunostaining was performed with Tau-G antibody (red), which recognizes uncleaved tau independently of its phosphorylation states (P– and P+) and with anti-dephosphorylated tau antibody, Tau-1 (green). Apoptotic neurons detected by nuclear staining with DAPI (A, arrows) were stained for dephosphorylated tau (Tau-1-positive) (B and D) but not with Tau-G antibody (C and D). Non-apoptotic neurons (A, arrowheads) did not display staining for dephosphorylated tau (B and D) but were positive for total tau (C and D). Scale bar: 8  $\mu$ m.

**Caspase Inhibition Prevents Abnormal Dephosphorylated Tau Distribution, Tau Cleavage, and Apoptosis**—To analyze the involvement of caspases in staurosporine-induced apoptosis, caspases were inhibited by Boc-D-FMK. Immunoblots with antibodies directed against phosphorylated tau (AT-8, AD-2, AT-180, and AT-270), against dephosphorylated tau (Tau-1) or against phospho-independent tau (T46, Tau-5, and Tau-G) confirmed that staurosporine reduced Tau FL levels as a consequence of tau cleavage and degradation (Fig. 6A). Inhibition of caspases by 50  $\mu$ M Boc-D-FMK effectively prevented the generation of the 15-kDa dephosphorylated tau fragment and restored dephosphorylated Tau FL as shown in Western blot using anti-dephosphorylated tau antibody, Tau-1 (Fig. 6A). Western blots using Tau-5 showed that no tau fragment was



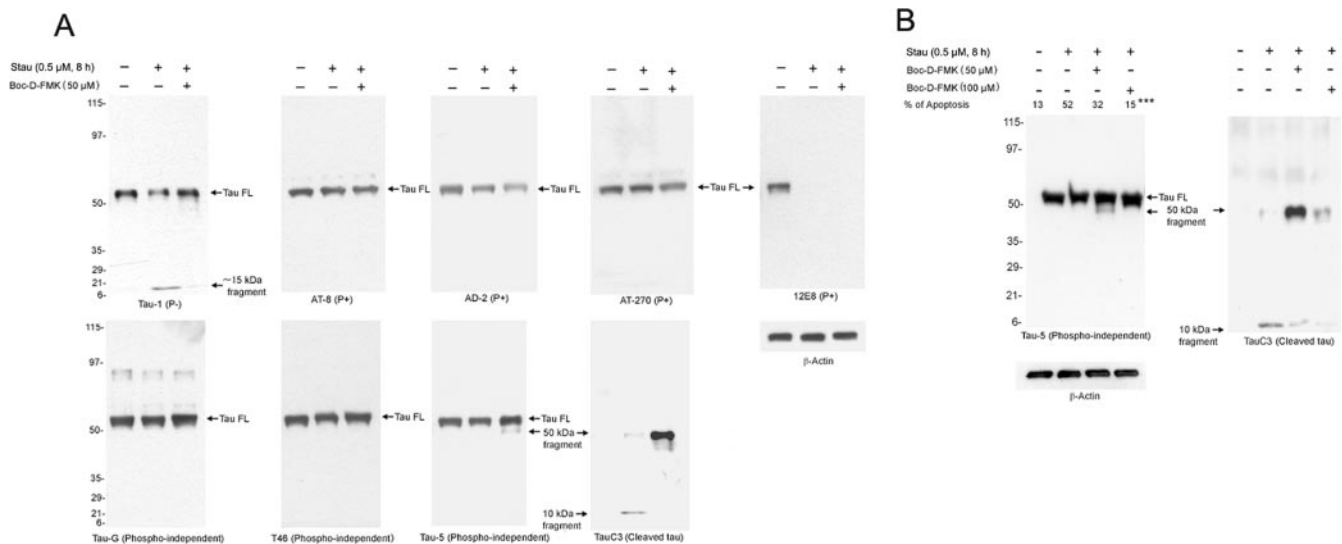


**FIG. 6. Effects of caspase inhibition on tau cleavage and apoptosis.** *A*, Western blots using anti-total tau antibodies Tau-5, Tau-G, and T46 show that staurosporine (*Stau*) decreased total tau. Phospho-dependent anti-tau antibodies revealed that staurosporine strongly decreased tau phosphorylated at AD-2 and 12E8 epitopes and to a lesser extent at AT-8 and AT-270 epitopes. TauC3 antibody detected the 10-kDa fragment and very low levels of the 50-kDa fragment. The 15 kDa was detected by Tau-1 antibody. Caspase inhibition by 50  $\mu$ M Boc-D-FMK blocked generation of the 10-kDa fragment, increased the amount of the 50-kDa fragment (Western blots with TauC3 and Tau-5 antibodies), prevented formation of the dephosphorylated 15-kDa fragment (Tau-1 Western blot), and restored dephosphorylated but not phosphorylated full-length tau (*Tau FL*) (see Western blots using Tau-1, AT-8, AD-2, AT-270, AT-180, Tau-5, Tau-G, and T46 antibodies). *B*, Western blot using Tau-5 and TauC3 antibodies confirming results shown in *A*. In addition, a higher Boc-D-FMK concentration (100  $\mu$ M) efficiently prevented the generation of 50- and 10-kDa fragments and apoptosis and completely restored *Tau FL* (TauC3 and Tau-5 Western blots). \*\*\*,  $p < 0.001$  compared with apoptosis in staurosporine-exposed cultures.

detected in control and staurosporine-exposed cultures, whereas inhibition of caspase by 50  $\mu$ M Boc-D-FMK led to the appearance of the 50-kDa fragment (Fig. 6*A*). The presence of the 50-kDa fragment in cultures exposed to staurosporine in the presence of 50  $\mu$ M Boc-D-FMK was confirmed by Western blot using anti-cleaved tau antibody TauC3. TauC3 detected the 10-kDa fragment and a few 50-kDa fragments in staurosporine-exposed cultures. Caspase inhibition prevented generation of the 10-kDa fragment and enhanced 50-kDa fragment generation. The increase in 50-kDa fragments due to partial caspase inhibition by 50  $\mu$ M Boc-D-FMK cannot result from additional tau cleavage, because *Tau FL* was restored. Moreover, extensive inhibition of caspases by 100  $\mu$ M Boc-D-FMK almost completely blocked the generation of tau fragments (50 and 10 kDa) (Fig. 6*B*). Inhibition of caspases by 100  $\mu$ M Boc-D-FMK also reduced staurosporine-induced apoptosis from 52% to 15% ( $p < 0.001$ ). Western blots using anti-phosphorylated tau antibodies showed that caspase inhibition did not modify phosphorylated tau levels in staurosporine-exposed neurons (Fig. 6*A*).

Analysis of Tau phosphorylation by immunostaining with Tau-1 and AT-8 antibodies revealed that caspase inhibition by 100  $\mu$ M Boc-D-FMK prevented abnormal dephosphorylated tau distribution but did not affect tau phosphorylation when compared with staurosporine alone (Fig. 4*C''*, see Western blot using AT-8 in Fig. 6*A*). Inhibition of caspases gave rise to non-apoptotic neurons with strong immunolabeling for dephosphorylated tau distributed both in cell bodies and neurites (Fig. 4*B''*). These experiments indicate that caspase blockade prevents tau cleavage and apoptosis without interfering with changes in tau phosphorylation induced by staurosporine.

**Prior Tau Dephosphorylation Enhances Neuron Vulnerability to Apoptosis and Tau Cleavage**—It was previously reported that, in differentiated PC12 cells, tau dephosphorylation at the Tau-1 epitope characterized the onset of the execution phase of apoptosis (20). If tau dephosphorylation is a key event in this phase, then prior tau dephosphorylation must lead to an acceleration of apoptosis and tau cleavage. To determine whether

tau dephosphorylation was involved in its cleavage and apoptosis, tau was dephosphorylated by a glycogen synthase kinase-3 $\beta$  inhibitor, lithium, and then exposed to 0.5  $\mu$ M staurosporine. Preincubation of cultures with LiCl induced tau dephosphorylation (at least at the Tau-1 epitope) without detectable tau cleavage (Fig. 7*A*) and apoptosis. Western blots using anti-dephosphorylated tau antibody, Tau-1, showed that a 3-h staurosporine exposure alone failed to induce detectable tau cleavage (Fig. 7*B*), whereas prior tau dephosphorylation potentiated staurosporine-induced tau cleavage and apoptosis. This potentiating effect was also reflected by a decrease in the levels of *Tau FL* detected by Tau-5 antibody (Fig. 7*B*).

To confirm the involvement of tau dephosphorylation in its cleavage and degradation, cultures were exposed to colchicine. Colchicine destabilizes the cytoskeleton by depolymerizing microtubules. Colchicine was reported to dephosphorylate tau (27) and to induce neuronal apoptosis (28). Western blot using Tau-1 antibody showed that 1  $\mu$ M colchicine induced tau dephosphorylation in a time-dependent manner (Fig. 8*A*). Western blots using anti-phosphorylated tau antibodies AT-8, AT-180, AT-270, AD-2, and 12E8 showed a decrease in phosphorylated tau immunoreactivities thereby confirming that colchicine induced tau dephosphorylation. As demonstrated for staurosporine treatment, colchicine exposure generated a 15-kDa dephosphorylated tau fragment following 12-h exposure. However, by contrast with what was seen with staurosporine, colchicine induced detectable levels of intermediate tau fragments, including a 50-kDa fragment. These fragments were mainly detected by Tau-1, T46, Tau-G, and Tau-5 antibodies. TauC3 detected two fragments smaller than 50 kDa (~40 and 45 kDa) following 8- and 12-h colchicine exposure (Fig. 8*A*). PP2A inhibition by okadaic acid (OKA) (25 and 50 nM) alone induced morphological changes such as neurite disruption without nuclear fragmentation and increased phosphorylated tau but failed to induce tau cleavage (data not shown). PP2A inhibition blocked colchicine-induced tau dephosphorylation and increased tau phosphorylation as shown by Western blots using AD2, 12E8, AT-180, AT-8, and AT270 antibodies

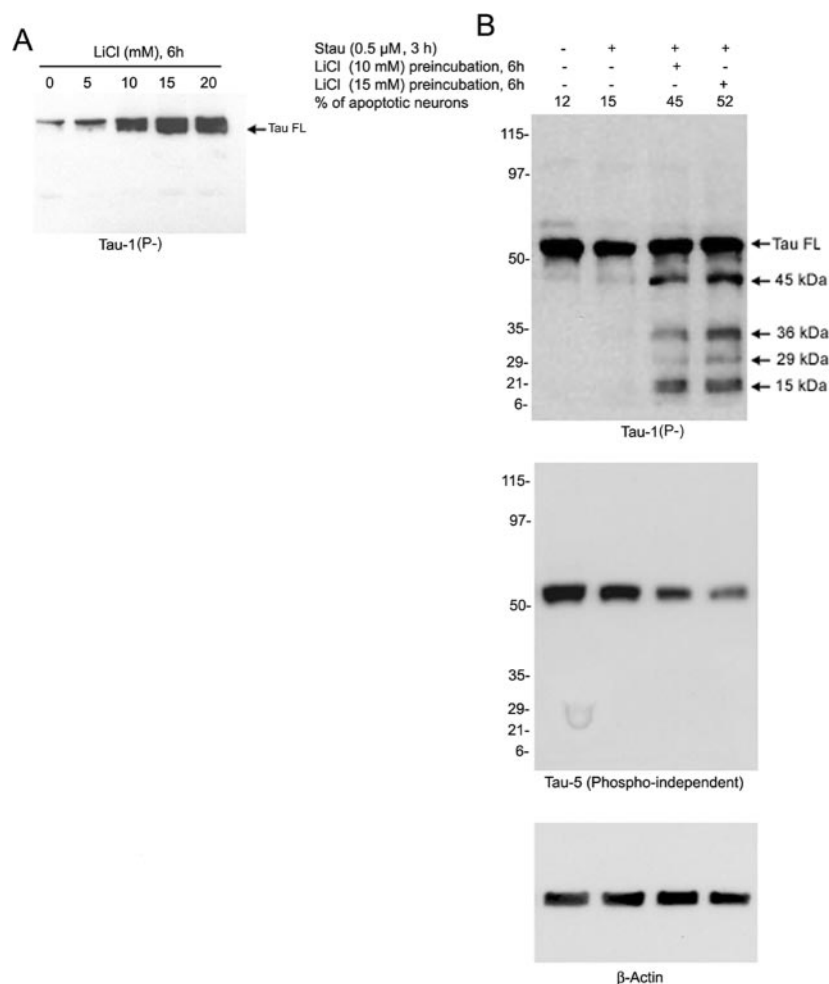


**FIG. 7. Prior tau dephosphorylation enhances its cleavage and increases neuron vulnerability to apoptosis.** *A*, lithium alone induced tau dephosphorylation at the Tau-1 epitope in a dose-dependent manner without cleavage. *B*, exposure to staurosporine alone (0.5  $\mu$ M, 3 h) induced minor apoptosis, and no tau fragment was observed (Western blot using Tau-1 antibody for dephosphorylated tau and Tau-5 antibody for total tau). Prior tau dephosphorylation (by lithium preincubation) potentiated the staurosporine-induced decrease in total tau and apoptosis with generation of high levels of dephosphorylated tau fragments.

and with anti-dephosphorylated tau antibody, Tau-1 (Fig. 8*B*). PP2A inhibition also blocked tau cleavage and restored Tau FL as shown by Western blots using antibodies directed against total tau, T46, Tau-G, and Tau-5 (Fig. 8*B*). In contrast to what was observed in cultures exposed to staurosporine, in cultures exposed to colchicine, caspase inhibition by 100  $\mu$ M Boc-D-FMK failed to restore Tau FL. Moreover, as shown in Western blots using TauC3 antibody, caspase inhibition also failed to prevent the generation of tau fragments (Fig. 8*B*). These data indicate that the patterns of tau cleavage and degradation are different in colchicine and staurosporine treatments. Western blots using TauC3 antibody also showed that PP2A inhibition by 25 nM OKA led to the appearance of an intense 50-kDa fragment that may correspond to phosphorylated forms of the 40- and 45-kDa fragments generated by colchicine treatment. This cannot result from an additional tau cleavage due to treatment with 25 nM OKA, because at this concentration the Tau FL was restored (see Western blot using antibody Tau-5 for example). In addition, extensive inhibition of PP2A by 50 nM OKA almost completely prevented the formation of the 50-kDa fragment.

#### DISCUSSION

In the present study we analyzed tau phosphorylation and cleavage during staurosporine-induced neuronal apoptosis. We also investigated the impact of tau dephosphorylation on its cleavage and apoptosis. Except for the 12E8 epitope Ser<sup>262</sup>/Ser<sup>356</sup>, we demonstrated that for all phospho-epitopes examined staurosporine induced an early (15-min exposure) and transient increase in tau phosphorylation. The peak increase in tau phosphorylation depended upon epitope analyzed and was obtained following 1 h of staurosporine treatment for the AT-8

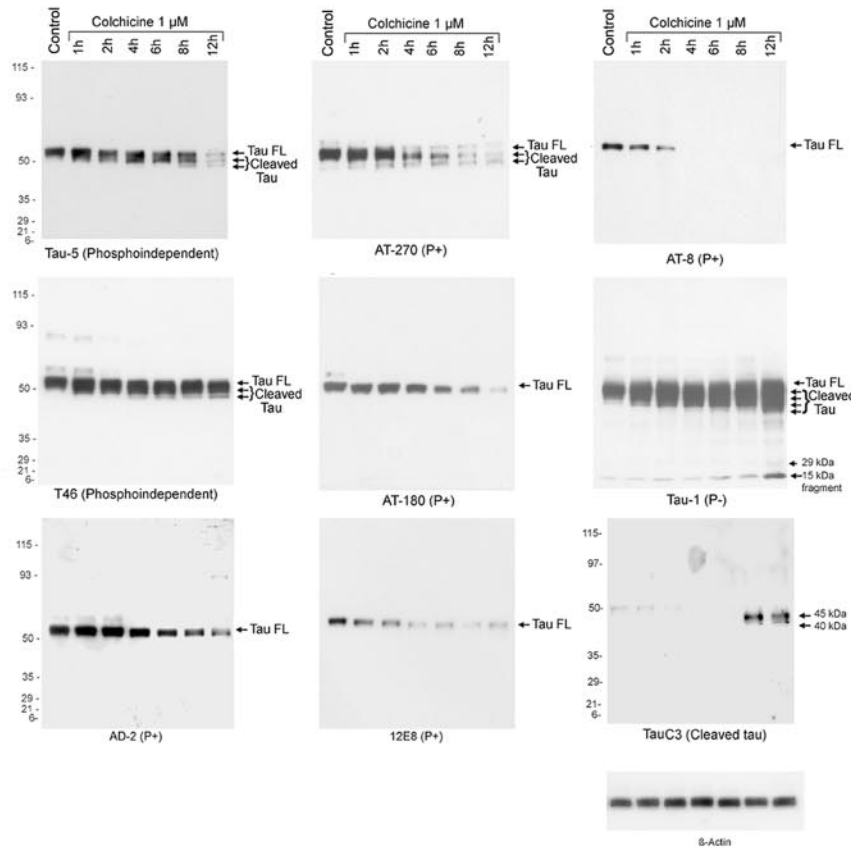
epitope Ser<sup>202</sup>/Thr<sup>205</sup> and 4 h for the AD-2 epitope Ser<sup>396</sup>/Ser<sup>404</sup>. These data indicate that interactions may exist between tau phosphorylation epitopes; phosphorylation of one epitope facilitates that of other epitopes.

Our findings are, in part, in agreement with those reported in NGF-deprived PC-12 cells by Zhang *et al.* (17). In that study, increases in tau phosphorylation were reported for 12E8, AT-8/Tau-1, and PHF-1 epitopes, whereas phosphorylation at the AT-270 epitope Thr<sup>181</sup> was unchanged. At the opposite, in our model of cultured primary neurons exposed to staurosporine, tau phosphorylation increased at AT-270 and decreased at 12E8. These discrepancies may be due to differences in culture models and the apoptosis triggers. Serine 356 is located in the MT-binding domain, and its phosphorylation only slightly reduced tau binding to microtubules (26, 23). In our study, staurosporine reduced tau binding to microtubules and decreased tau phosphorylation at serines 262 and 356. If we consider that decreased tau binding (due to tau phosphorylation) to microtubules is a key event in our model of apoptosis, the involvement of tau phosphorylation at serines 262 and 356 in neuronal apoptosis can be excluded.

Gamblin *et al.* (24) and Chung *et al.* (30) demonstrated that tau cleavage occurs during neuronal apoptosis of cultured neurons. Using an acellular system, these authors also demonstrated that recombinant tau protein could be cleaved by caspase-3 at Asp<sup>421</sup>. This cleavage led to a 50-kDa fragment that encompasses residues 1–421. Both studies showed that Tau-5 antibody detected the 50-kDa fragment. This antibody reacts with residues 210–230 of tau independently of its phosphorylation states. This fragment was also specifically detected



**A**



**B**

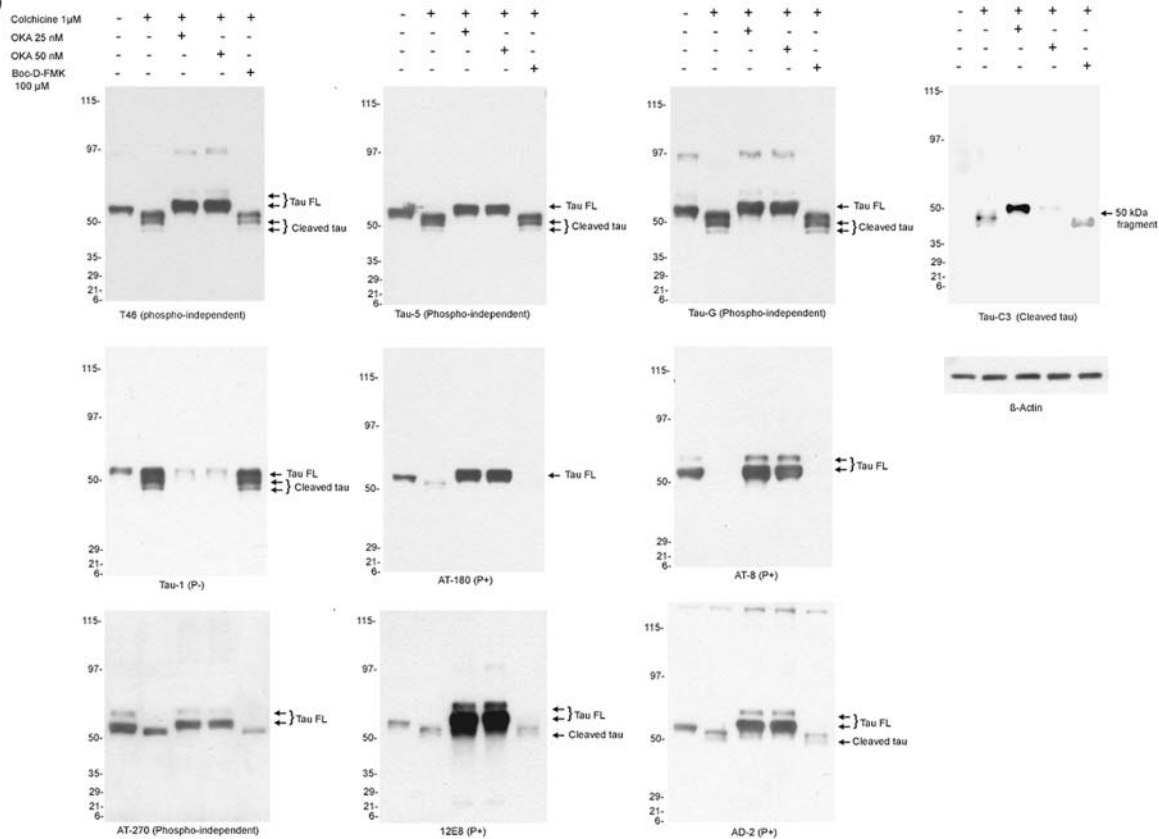


**FIG. 8. Colchicine induces tau dephosphorylation and cleavage which are blocked by PP2A inhibition.** A, Western blot analysis using anti-phosphorylated tau antibodies (AT-180, AT-270, AT-8, AD-2, and 12E8) shows decreased phosphorylated tau during colchicine treatment. In parallel, colchicine increased dephosphorylated tau (at the Tau-1 epitope) and generated a laddering of dephosphorylated tau fragments that included the 15-kDa fragment. AT-270 antibodies detected few 50-kDa fragments. Antibodies directed against phosphorylation-independent tau

by TauC3, a monoclonal antibody directed against residues 412–421 (24). In our study, when protein extraction was carried out with modified Laemmli sample buffer, anti-phosphorylated tau antibodies and Tau-5 antibody only detected very low levels of tau fragments (45 and 50 kDa) during staurosporine-induced apoptosis compared with results obtained by Chung *et al.* and Gamblin *et al.* However, only the anti-dephosphorylated tau antibody Tau-1 and the anti-cleaved tau antibody TauC3 detected tau fragments. In addition to the 50-kDa fragment reported by Gamblin *et al.*, TauC3 detected a 10-kDa fragment. Additional experiments carried out to explain these discrepancies showed that, depending on the extraction buffer used, the 50-kDa fragment can be easily detected in staurosporine-exposed cultures by TauC3 and Tau-5 antibodies as previously described (24, 30). We also demonstrated that when caspases were inhibited during tau fractionation, generation of the 50-kDa tau fragment was abolished. These data indicate that the 50-kDa tau fragment can be generated during fractionation. Apoptosis detection often relies on assays based on the ability of caspases to cleave specific protein substrates. Because protein substrate cleavage by caspases may occur during extraction, it is therefore important to inhibit caspases to avoid overestimation of substrate cleavage.

We were unable to easily detect the 50-kDa fragment in the total fraction merely because its levels were too low. In fact, partial inhibition of caspases was inhibited by 50  $\mu$ M Boc-D-FMK blocked formation of the 10-kDa fragment and enhanced the 50-kDa fragment. This indirectly indicates that the 50-kDa fragment was indeed generated in our model and may explain differences between our results and those of Chung *et al.* and Gamblin *et al.* Possibly the 50-kDa fragment is kept at low levels, because it is rapidly degraded into smaller fragments, mainly the 10- and 15-kDa fragments. Therefore, the 50-kDa fragment cannot accumulate in dying cells unless the proteolytic systems responsible for its degradation are overcome.

Tau possesses at least two caspase-3 cleavage sites located in <sup>345</sup>DFKD<sup>348</sup> and <sup>418</sup>DMVD<sup>421</sup> tetrapeptides. Chung *et al.* (30) and Gamblin *et al.* (24) showed that caspases cleaved tau only at Asp<sup>421</sup> leading to a 50-kDa fragment. In our study, the 10-kDa fragment detected by TauC3 may result from an additional cleavage at Asp<sup>348</sup>. This would generate a fragment spanning residues 349–421 (73 amino acids) having a calculated molecular mass of ~8.8 kDa, which may represent the 10-kDa fragment observed in Western blots. These data establish that in cultured neurons, caspases cleave tau not only at Asp<sup>421</sup> but also probably at Asp<sup>348</sup>.

As previously reported (18–20), examination of individual neurons showed that the majority of apoptotic neurons (neurons with fragmented nuclei) exclusively displayed dephosphorylated tau at least at the Tau-1 epitope. In these neurons, immunostaining for dephosphorylated tau was found in cell bodies and degenerating axons. In addition, we demonstrated that alterations in dephosphorylated tau localization were due to tau cleavage and not to tau dephosphorylation.

We confirmed previous reported results (18) showing that caspase inhibition prevented tau cleavage and apoptosis. In addition, we found that protected neurons were strongly stained for dephosphorylated tau. This staining was uniformly

distributed in cell bodies and neuronal processes. Western blot analysis showed that caspase inhibition restored full-length dephosphorylated tau without altering tau phosphorylation. These data clearly indicate that caspase inhibition blocked tau cleavage without reversing tau dephosphorylation.

In our experimental model, tau dephosphorylation is required for its cleavage and degradation, because: 1) Anti-phosphorylated tau antibodies failed to detect significant fragmented tau both in staurosporine and colchicine-exposed cultures; 2) In staurosporine-exposed cultures, if caspases cleaved phosphorylated tau, then their inhibition would restore full-length phosphorylated tau. This was not clearly the case, because, on the contrary, caspase inhibition restored full-length dephosphorylated tau; 3) Prior tau dephosphorylation by lithium potentiated staurosporine-induced tau cleavage and apoptosis; and 4) Colchicine induced tau dephosphorylation and cleavage/degradation. Both phenomena were prevented by inhibition of PP2A. For these reasons, we can conclude that tau must be dephosphorylated to be cleaved and degraded.

How does tau dephosphorylation enhance neuron vulnerability to apoptosis and tau cleavage? Chronic exposure to lithium was previously reported to induce neuronal apoptosis in juvenile cultured neurons (32). An explanation for this neurotoxic effect might be that tau dephosphorylation enhances tau cleavage induced by an apoptotic trigger (demonstrated in our study), which in turn generates toxic tau fragments (30). However, lithium might also interfere with intracellular transduction pathways upstream from tau dephosphorylation, tau cleavage, and apoptosis.

Our study does not determine whether or not modifications in tau phosphorylation are directly involved in tau processing during neuronal apoptosis. The effect of PP2A inhibition on tau cleavage was not tested on staurosporine-induced tau cleavage and apoptosis, because both PP2A inhibition and staurosporine (in early stages of apoptosis) led to increased tau phosphorylation. The concomitant use of these two substances should lead to enhanced apoptosis. Additional experiments are needed to see whether tau phosphorylation or dephosphorylation directly alters its cleavage and degradation in a cell-free system.

PP2A inhibition led to increased levels of tau phosphorylated at all phospho-epitopes analyzed. Phosphorylation epitopes directly implicated in caspase-operated cleavage and subsequent degradation should be determined.

In our study PP2A inhibition prevented colchicine-induced tau dephosphorylation and cleavage/degradation. These results support recent findings demonstrating that tau-PHF decreased proteasome activity in AD brains (33) and that PHF injected into neurons required tau dephosphorylation before being degraded (34).

Tau is hyperphosphorylated during fetal brain development (35), in adult brain in response to wide a range of insults (for review, see Ref. 36) and in pathological conditions such as AD (7). Tau, in its hyperphosphorylated form, is the major component of PHF observed in AD (8, 9). During fetal brain development tau hyperphosphorylation plays an important role in neurogenesis where large levels of tau proteins are required. Tau hyperphosphorylation may protect tau from proteolysis thereby enhancing available tau levels

epitopes, Tau-5 and T46, detected intermediate tau fragments with molecular masses ranging from 40 to 50 kDa. Anti-cleaved tau antibody TauC3 detected 40- and 45-kDa fragments following 8- and 12-h colchicine exposure. *B*, effects of PP2A inhibition by OKA and caspase inhibition by Boc-D-FMK on tau dephosphorylation and cleavage induced by colchicine. Western blot using phospho-dependent anti-tau antibodies (AT-180, AT-270, AT-8, AD-2, 12E8, and Tau-1) showed that PP2A inhibition but not caspase inhibition reversed colchicine-induced tau dephosphorylation, leading to increased tau phosphorylation at all epitopes examined. Colchicine-induced tau cleavage and degradation were also prevented by PP2A inhibition but not by caspase inhibition (Western blots using anti-total tau antibodies Tau-5, T46, and Tau-G and anti-dephosphorylated tau antibody, Tau-1). TauC3 antibody showed that PP2A inhibition by 25 nM OKA during colchicine exposure led to the accumulation of the 50-kDa fragment, whereas 50 nM OKA potentially prevented the generation of tau fragments.

needed for neurogenesis. Tau hyperphosphorylation decreases its capacity to interact with microtubules. It is possible that, during brain development, tau must be dephosphorylated at least at epitopes involved in this interaction to be able to bind to microtubules. Levels of dephosphorylated tau should correspond to those of available microtubules. Excess dephosphorylated tau accumulates in neurons. This accumulation can be obtained experimentally by exposing cultured neurons to lithium. Dephosphorylated tau itself is not deleterious for neurons. However, as shown here, in the presence of a trigger, tau dephosphorylation facilitates its cleavage and degradation and accelerates apoptosis.

In adult animal brains, stress-induced tau hyperphosphorylation seems to be an adaptation to new environmental conditions. In fact, Arendt *et al.* (37) recently reported the formation of highly phosphorylated tau at several PHF-like epitopes in torpor during hibernation. This PHF-like phosphorylation was fully reversible after arousal. The authors suggested that repeated formation of PHF-like tau might represent a physiological mechanism not necessarily associated with pathological effects. In contrast, in AD brains tau hyperphosphorylation cannot be reversed and contributes to the formation of PHF. Therefore, the down-regulation of PP2A activity reported in AD brains (38) might contribute to the accumulation of highly phosphorylated tau into PHF as a result not only of hyperphosphorylation but also to the inhibition of cleavage and degradation in degenerating neurons. In conclusion, dephosphorylation plays a crucial role not only in facilitating tau binding to microtubules during brain development and neuronal plasticity, but also in clearing highly phosphorylated tau observed in degenerating neurons to prevent the formation of PHF.

**Acknowledgments**—We thank Dr. V. M.-Y. Lee, Dr. C. Mourtou-Gilles, Dr. P. Seubert, and Prof. L. I. Binder for providing us, respectively, with T46, AD-2, 12E8, and TauC3 antibodies. We also thank Dr. J. Cook-Moreau and Dr. Didier Pelaprat for helpful comments on the manuscript.

#### REFERENCES

- Binder, L. I., Frankfurter, A., and Rebhun L. I. (1985) *J. Cell Biol.* **101**, 1371–1378
- Johnson, G. V., and Jenkins, S. M. (1999) *J. Alzheimers Dis.* **1**, 307–328
- Jameson, L., Frey, T., Zeeberg, B., Dalldorf, F., and Caplow, M. (1980) *Biochemistry* **19**, 2472–2479
- Lindwall, G., and Cole, R. D. (1984) *J. Biol. Chem.* **259**, 5301–5305
- Tanaka, T., Zhong, J., Iqbal, K., Trenkner, E., and Grundke-Iqbal, I. (1998) *FEBS Lett.* **426**, 248–254
- Baum, L., Seger, R., Woodgett, J. R., Kawabata, S., Maruyama, K., Koyama, M., Silver, J., and Saitoh, T. (1995) *Brain Res. Mol. Brain Res.* **34**, 1–17
- Lee, V. M., Balin, B. J., Otvos, L., Jr., and Trojanowski, J. Q. (1991) *Science* **251**, 675–678
- Greenberg, S. G., Davies, P., Schein, J. D., and Binder, L. I. (1992) *J. Biol. Chem.* **267**, 564–569
- Sergeant, N., David, J. P., Goedert, M., Jakes, R., Vermersch, P., Buee, L., Lefranc, D., Watzet, A., and Delacourte, A. (1997) *J. Neurochem.* **69**, 834–844
- McCarthy, M. J., Rubin, L. L., and Philpott, K. L. (1997) *J. Cell Sci.* **110**, 2165–2173
- Martinou, J. C., and Sadoul, R. (1996) *Curr. Opin. Neurobiol.* **6**, 609–614
- Salvesen, G. S., and Dixit, V. M. (1997) *Cell* **91**, 443–446
- Brancolini, C., Benedetti, M., and Schneider, C. (1995) *EMBO J.* **14**, 5179–5190
- Martin, S. J., O'Brien, G. A., Nishioka, W. K., McGahon, A. J., Mahboubi, A., Saido, T. C., and Green, D. R. (1995) *J. Biol. Chem.* **270**, 6425–6428
- Levee, M. G., Dabrowska, M. I., Lelli, J. L., Jr., and Hinshaw, D. B. (1996) *Am. J. Physiol.* **271**, 1981–1992
- Davis, P. K., and Johnson, G. V. (1999) *J. Biol. Chem.* **274**, 35686–35692
- Zhang, J., and Johnson, G. V. (2000) *J. Neurochem.* **75**, 2346–2357
- Canu, N., Dus, L., Barbato, C., Ciotti, M. T., Brancolini, C., Rinaldi, A. M., Novak, M., Cattaneo, A., Bradbury, A., and Calissano, P. (1998) *J. Neurosci.* **18**, 7061–7074
- Lesort, M., Blanchard, C., Yardin, C., Esclaire, F., and Hugon, J. (1997) *Brain Res. Mol. Brain Res.* **45**, 127–132
- Mills, J., Lee, V. M., and Pittman, R. N. (1998) *J. Cell Sci.* **111**, 625–636
- Goedert, M., Spillantini, M. G., Jakes, R., Rutherford, D., and Crowther, R. A. (1989) *Neuron* **3**, 519–526
- Buee-Scherrer, V., Buee, L., Hof, P. R., Leveugle, B., Gilles, C., Loerzel, A. J., Perl, D. P., and Delacourte, A. (1995) *Am. J. Pathol.* **146**, 924–932
- Seubert, P., Mawal-Dewan, M., Barbour, R., Jakes, R., Goedert, M., Johnson, G. V., Litsky, J. M., Schenk, D., Lieberburg, I., Trojanowski, J. Q., and Lee, V. M.-Y. (1995) *J. Biol. Chem.* **270**, 18917–18922
- Gamblin, T. C., Chen, F., Zambrano, A., Abrahams, A., Lagalwar, S., Guillozet, A. L., Lu, M., Fu, Y., Garcia-Sierra, F., LaPointe, N., Miller, R., Berry, R. W., Binder, L. I., and Cryns, V. L. (2003) *Proc. Natl. Acad. Sci. U. S. A.* **100**, 10032–10037
- Terro, F., Esclaire, F., Yardin, C., and Hugon, J. (2000) *Neurosci. Lett.* **278**, 149–152
- Boix, J., Llecha, N., Yuste, V. J., and Comella, J. X. (1997) *Neuropharmacology* **36**, 811–821
- Merrick, S. E., Demoise, D. C., and Lee, V. M. (1996) *J. Biol. Chem.* **271**, 5589–5594
- Bonfoco, E., Ceccatelli, S., Manzo, L., and Nicotera, P. (1995) *Exp. Cell Res.* **218**, 189–200
- Jenkins, S. M., Zinnerman, M., Garner, C., and Johnson, V. W. (2000) *Biochem. J.* **275**, 263–270
- Chung, C. W., Song, Y. H., Kim, I. K., Yoon, W. J., Ryu, B. R., Jo, D. G., Woo, H. N., Kwon, Y. K., Kim, H. H., Gwag, B. J., Mook-Jung, I. H., and Jung, Y. K. (2001) *Neurobiol. Dis.* **8**, 162–172
- Litsky, J. M., Johnson, G. V., Jakes, R., Goedert, M., Lee, M., and Seubert, P. (1996) *Biochem. J.* **316**, 655–660
- D'Mello, S. R., Anelli, R., and Calissano, P. (1994) *Exp. Cell Res.* **211**, 332–338
- Keck, S., Nitsch, R., Grune, T., and Ullrich, O. (2003) *J. Neurochem.* **85**, 115–122
- Hall, G. F. (1999) *J. Alzheimers Dis.* **1**, 379–386
- Mawal-Dewan, M., Henley, J., Van de Voorde, A., Trojanowski, J. Q., and Lee, V. M. (1994) *J. Biol. Chem.* **269**, 30981–30987
- Yen, S. H., Liu, W. K., Hall, F. L., Yan, S. D., Stern, D., and Dickson, D. W. (1995) *Neurobiol. Aging* **16**, 381–387
- Arendt, T., Stieler, J., Strijkstra, A. M., Hut, R. A., Rüdiger, J., Van der Zee, E. A., Harkany, T., Holzer, M., and Hortig, W. (2003) *J. Neurosci.* **23**, 6972–6981
- Trojanowski, J. Q., and Lee, V. M. (1995) *FASEB J.* **9**, 1570–1576